Acceleron Aerospace Journal || AAJ.11.2106-2465
Volume 3, Issue 6, pp (648-669)
Research Paper
E-ISSN- 2583-9942 || DOI: 10.61359/11.2106-2465

Expression of Complete Elliptic Integrals of the First and Second Kind in Terms of Elementary Functions in the Tunnel Mathematics Space

Oleh G. Shvydkyi *

Independent Researcher, Zaporizhzhia, Ukraine

Abstract: Analytical expressions in closed form of complete elliptic integrals of the first and second kind are obtained in terms of elementary functions. These expressions model the tabular values of integrals quite well, so they can be used for differentiation and integration, as well as for solving certain applied problems. When deriving these expressions in tunnel mathematics space, an additional dependence on the azimuthal angle φ as a parameter appears. Precise adjustment of this parameter allows reducing the error in modeling.

Table of Contents

1. Introduction

In mathematics, some goals are unachievable by conventional methods. One such goal is to represent complete elliptic integrals of the first and second kind in term of elementary functions. A new mathematical tool will be effective only if it can solve such a problem. As we will see below, the use of the apparatus of tunnel mathematics, based on the spatial theory of functions of a complex variable, allows us to achieve success.

2. Brief concepts

2.1. Incomplete and complete elliptic integral of the first kind

The incomplete elliptic integral of the first kind F [2, 3, 4, 5, 7, 8, 9] is defined as

$$F(z,k) = \int_0^z \frac{dz}{\sqrt{1-(k\sin z)^2}}; \tag{1}$$

where

$$0 < z < \frac{\pi}{2}. \tag{2}$$

This is Legendre's trigonometric form of the elliptic integral.

In expression (1) z is the amplitude; k is the elliptic modulus.

Elliptic integrals are said to be 'complete' when the amplitude $z = \frac{\pi}{2}$. The complete elliptic integral of the first kind K may thus be defined as

*Research Scholar, Independent Researcher, Zaporizhzhia, Ukraine. **Corresponding Author: oleg.shv.jw@gmail.com**
** Received: 20-November-2024 || Revised: 26-November-2024 || Accepted: 28-November-2024 || Published Online: 30-November-2024.

$$K(k) = \int_0^{\frac{\pi}{2}} \frac{dz}{\sqrt{1-(k\sin z)^2}}; \quad (3)$$

or more compactly in terms of the incomplete integral of the first kind as

$$K(k) = F\left(\frac{\pi}{2}, k\right). \quad (4)$$

Plot of the complete elliptic integral of the first kind *K(k)* **[11, 1,]** is shown on Fig. 1.

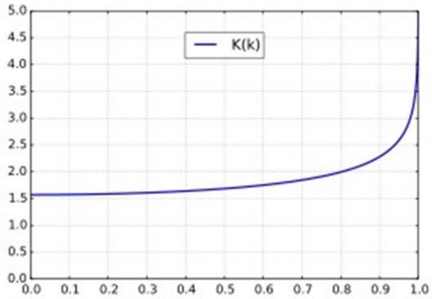

Figure-1. Plot of the complete elliptic integral of the first kind *K(k)*.

The complete elliptic integral of the first kind can be expressed as a power series **[6, 10]**

$$K(k) = \frac{\pi}{2}\sum_{n=0}^{\infty}\left(\frac{(2n)!}{2^{2n}(n!)^2}\right)^2 k^{2n} = \frac{\pi}{2}\left(1 + \left(\frac{1}{2}\right)^2 k^2 + \left(\frac{1\cdot 3}{2\cdot 4}\right)^2 k^4 + \cdots + \left(\frac{(2n-1)!!}{(2n)!!}\right)^2 k^{2n} + \cdots\right); \quad (5)$$

where n!! denotes the double factorial.

The complete elliptic integral of the first kind can be computed very efficiently in terms of the arithmetic–geometric mean **[1, 8]**.

2.2. Incomplete and complete elliptic integral of the second kind

The incomplete elliptic integral of the second kind E [2, 3, 4, 5, 7, 8, 9] in Legendre's trigonometric form is

$$E(z,k) = \int_0^{z} \sqrt{1-(k\sin z)^2}\, dz; \quad (6)$$

where $0 < z < \frac{\pi}{2}$.

The complete elliptic integral of the second kind *E* is defined as

$$E(k) = \int_0^{\frac{\pi}{2}} \sqrt{1-(k\sin z)^2}\, dz; \quad (7)$$

or more compactly in terms of the incomplete integral of the second kind as

$$E(k) = E\left(\frac{\pi}{2}, k\right). \quad (8)$$

Plot of the complete elliptic integral of the second kind *E(k)* **[11, 1,]** is shown on Fig. 2.

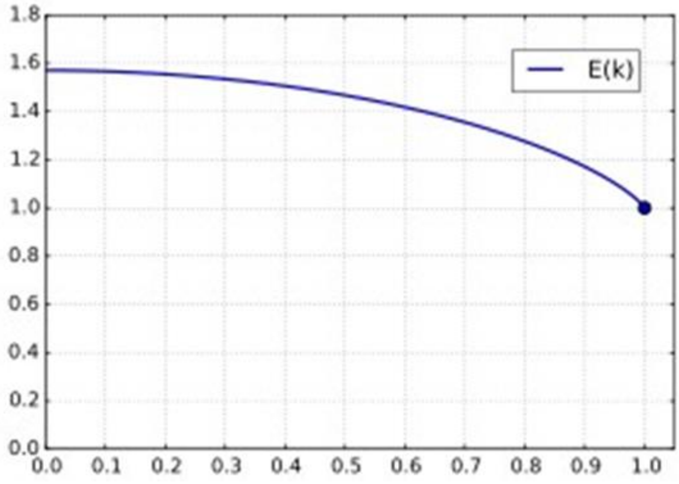

Figure-2. Plot of the complete elliptic integral of the second kind *E(k)*.

The complete elliptic integral of the second kind can be expressed as a power series **[6, 10]**

$$E(k) = \frac{\pi}{2}\sum_{n=0}^{\infty}\left(\frac{(2n)!}{2^{2n}(n!)^2}\right)^2 \frac{k^{2n}}{1-2n} = \frac{\pi}{2}\left(1 - \left(\frac{1}{2}\right)^2 \frac{k^2}{1} - \left(\frac{1\cdot 3}{2\cdot 4}\right)^2 \frac{k^4}{3} - \cdots - \left(\frac{(2n-1)!!}{(2n)!!}\right)^2 \frac{k^{2n}}{2n-1} - \cdots\right); \quad (9)$$

Like the integral of the first kind, the complete elliptic integral of the second kind can be computed very efficiently using the arithmetic–geometric mean **[1, 8]**.

In general, complete elliptic integrals of the first and second kind are not expressed in terms of elementary functions. If this happens, then integrals (3) and (7) are called pseudo-elliptic.

3. Theory

3.1. Definition of a spatial complex number

Similar to how a vector is defined in three-dimensional space, we define a spatial complex number as follows **[13]**:

$$L = ReL + iImL + fFantL = x + iy + fz. \quad (10)$$

Where *ReL* is a real part of a spatial complex number *L*, *ImL* is its imaginary part, *FantL* is its spatial part.

The spatial complex number *L* is shown in Fig. 3. We measure polar angle θ from *xy*-plane, not from *z*-axis, as usually.

The components of the spatial vector expressed in terms of its magnitude *R* as well as the azimuthal angle φ and the polar angle θ are defined as follows:

$$x = R\ \cos\theta \cos\varphi,$$
$$y = R\ \cos\theta \sin\varphi, \quad (11)$$
$$z = R\ \sin\theta.$$

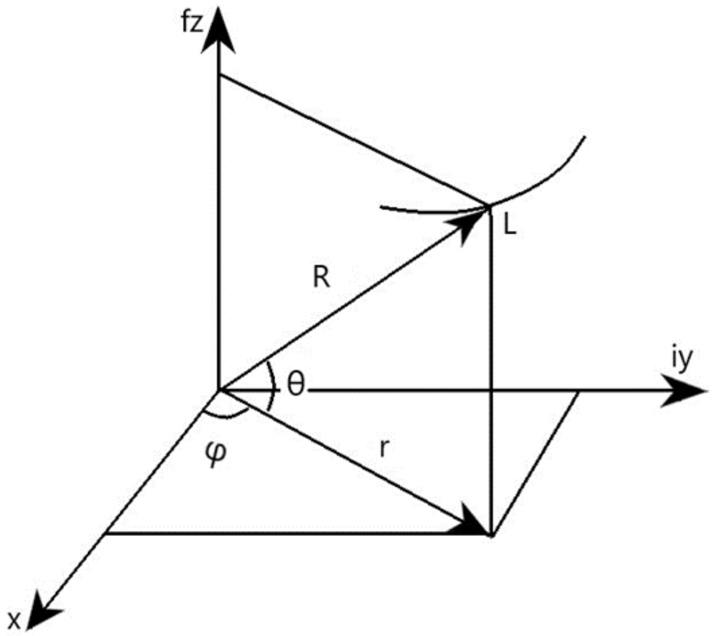

Figure-3. Spatial complex number *L*.

On the other hand, the following obvious equality holds

$$e^{i(\varphi+\theta)} = e^{i\varphi}e^{i\theta} = \cos\theta\cos\varphi + i\,cos\theta\ sin\varphi + ie^{i\varphi}sin\theta. \quad (12)$$

Now, if we introduce the operator

$$f = ie^{i\varphi} = e^{i(\varphi+\frac{\pi}{2})}, \quad (13)$$

then on the right-hand in (12) we obtain the expansion of the spatial vector with unit modulus along the *x*-, *y*-, *z*-axes. The components of this expansion coincide with the values of the projections in formula (11) at $R = 1$.

So, the spatial complex number is given by formula (10) where *x*, *y*, *z* are the real numbers.

The exponential form of the spatial complex number is

$$L = Re^{i\varphi+i'\theta} = Rexp[i\varphi + i'\theta] = Rexp[i\varphi + fexp[-i\varphi]\theta] = Rexp[i\varphi + f^*exp[i\varphi]\theta], \quad (14)$$

where i is an imaginary unit in *xy*-plane, i' is an imaginary unit in the plane that is perpendicular to *xy*-plane and contain *fz*-axes (Fig. 3); f is taken from (13) and f^* is taken from (21).

When deriving (14), the following expression was taken into account for i':

$$i' = fexp[-i\varphi] = f^*exp[i\varphi]. \quad (15)$$

From (15) we obtain simple relation between imaginary units i and i':

$$i = \frac{1}{\varphi}\log\frac{f}{i'}; \quad (16)$$

In form, (16) is similar to the expression for the Lyapunov characteristic indices **[14]**

$$L_s = \lim_{t\to\infty}\frac{1}{t}\log\frac{l_s(t)}{l(0)}, \quad (17)$$

where t is a time; $l_s(t)$ denotes the lengths of the semi-axes of the ellipsoid volume element into which the original spherical volume element transforms as it moves along its path in phase space of states; $l(0)$ is the radius of the original sphere, at a time arbitrarily chosen as $t = 0$.

The trigonometric form of the spatial complex number is

$$L = R(\cos\theta\cos\varphi + i\cos\theta\sin\varphi + f\sin\theta). \tag{18}$$

Using (14) and (18) we obtain an analogue of Euler's relation [12] in tunnel mathematics:

$$exp[i\varphi + f exp[-i\varphi]\theta] = \cos\theta\cos\varphi + i\cos\theta\sin\varphi + f\sin\theta. \tag{19}$$

We define the conjugate spatial complex number as follows:

$$L^* = x - iy - f^* z = Re^{-i(\varphi+\theta)}, \tag{20}$$

where $f^* = ie^{-i\varphi}$, (21)

hence taking into account (13) we have $f \cdot f^* = -1$. (22)

Identical to the planar theory the following relation holds

$$L \cdot L^* = R^2 = x^2 + y^2 + z^2. \tag{23}$$

Meanwhile the following relationships hold

$i^2 = -1$ (as in planar theory [12]);

$$i \cdot f = f \cdot i = -e^{i\varphi} = -\cos\varphi - i\sin\varphi = -\frac{x+iy}{\sqrt{x^2+y^2}}. \tag{24}$$

$$f^* = ie^{-i\varphi} = \sin\varphi + i\cos\varphi = \frac{y+ix}{\sqrt{x^2+y^2}} = f + 2\sin\varphi = f + \frac{2y}{\sqrt{x^2+y^2}}. \tag{25}$$

$$f^2 = -e^{2i\varphi} = -(\cos 2\varphi + i\sin 2\varphi) = -\frac{x^2-y^2+2ixy}{x^2+y^2}. \tag{26}$$

Considering that $f = ie^{i\varphi} = -\sin\varphi + i\cos\varphi = \frac{-y+ix}{\sqrt{x^2+y^2}}$, (27)

we can define spatial complex number on a plane as follows:

$$L = x\left(1 - \frac{yz}{x\sqrt{x^2+y^2}}\right) + iy\left(1 + \frac{xz}{y\sqrt{x^2+y^2}}\right). \tag{28}$$

3.2. Preparation of mathematical tools for integrating elliptic integrals

Now, using Euler's relation, we expand the left-hand side of (19), and then equate the components of this expansion to the corresponding components of the right-hand side of (19). This leads us to the following relations:

$$e^{f\theta\cos\varphi}\cos(f\theta\sin\varphi) = \cos\theta; \tag{29}$$

$$e^{f\theta\cos\varphi}\cos\varphi\sin(f\theta\sin\varphi) = 0; \tag{30}$$

$$e^{f\theta\cos\varphi}\sin\varphi\sin(f\theta\sin\varphi) = f\sin\theta; \tag{31}$$

From relations (29) and (31) we easily obtain

$$\tan(f\theta\sin\varphi) = \frac{f\tan\theta}{\sin\varphi}; \tag{32}$$

Now we square (29) and (31) and add the resulting expressions taking into account (32). This gives us our basic mathematical tool for integrating elliptic integrals:

$$e^{f\theta\cos\varphi} = |\cos\theta|\sqrt{\tan^2(f\theta\sin\varphi)+1}; \tag{33}$$

where $|\cos\theta|$ denotes the modulus of the function $\cos\theta$.

The expression under the square root on the right-hand side of (33) is very similar to the multiplier in the integrands in (3) and (7). We will use this to integrate complete elliptic integrals in the space of tunnel mathematics.

In the tunnel mathematics space, it is very convenient to perform integration over the

z-coordinate, since the operator *f* in (27) does not depend on this coordinate:

$$\int e^{fz}\,dz = \frac{1}{f}\int e^{fz}\,d(fz) = -f^{*}e^{fz} + C. \tag{34}$$

In writing (34), we applied (22); *C* is the integration constant.

To take advantage of this, we rewrite (32) and (33) as follows:

$$\tan(fz) = f\,\frac{\tan\left(\frac{z}{\sin\varphi}\right)}{\sin\varphi} = fz'. \tag{35}$$

Expression (35) allows us to conclude that applying the tangent operation to the values on the *fz*-axis in the space of tunnel mathematics (Fig. 3) is equivalent to moving along this axis to a parallel plane.

$$e^{fz} = \left|\cos\left(\frac{z}{\cos\varphi}\right)\right|\sqrt{\tan^2(fz\tan\varphi)+1}. \tag{36}$$

Now we will find out the area of applicability of expressions (35) and (36) in the tunnel mathematics space. For this we will use expression (30). Obviously, (35) and (36) apply on the *xy*-plane ($\theta = 0$, Fig. 3), on the *z*-axis $\left(\theta = \pm\frac{\pi}{2}\right)$, and also on some lines or filaments in this space. To find the equations of these filaments, it is necessary to equate the expression under the root in (36) to zero.

$$\tan^2(fz\tan\varphi) = -1, \tag{37}$$

whence

$$\tan(fz\tan\varphi) = \pm\, i. \tag{38}$$

Of particular interest is the case when there is a '+' sign on the right-hand side of (38). Hence

$$fz\tan\varphi = \mathrm{Arctan}\, i = -\frac{i}{2}\mathrm{Log}\frac{i-i}{i+i} = -\frac{i}{2}\mathrm{Log}\,0 = -\frac{i}{2}\big(\log 0 + i(\varphi \ \pm 2\pi n)\big) = \frac{\varphi}{2} \pm \pi n + i\infty. \tag{39}$$

In (39) *n* is an integer.

Considering that

$$fz\tan\varphi = -z\frac{\sin^2\varphi}{\cos\varphi} + iz\sin\varphi, \tag{40}$$

(here we used (27)) we come to the following conditions:

$$z\sin\varphi = \infty, \tag{41}$$

which corresponds to the infinitely distant plane in Fig. 3;

and

$$-z\frac{\sin^2\varphi}{\cos\varphi}=\frac{\varphi}{2}\pm\pi n, \tag{42}$$

whence

$$z=-\frac{\cos\varphi}{\sin^2\varphi}\left(\frac{\varphi}{2}\pm\pi n\right). \tag{43}$$

The plots of function (43) for $n=0$ and $n=-1$ are shown in Figs. 4 and 5.

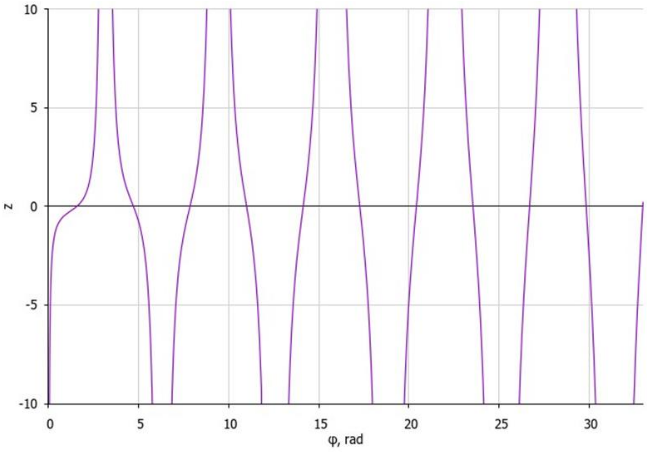

Figure-4. The plots of function (43) for $n=0$.

The lines shown in Figs. 4 and 5 correspond to certain lines or filaments in the space of tunnel mathematics, on which, in addition to the *xy*-plane and *z*-axis, relations (35) and (36) are fulfilled. As the azimuthal angle φ increases, these filaments become completely periodic. As we will see below, these conditions are quite sufficient for the analytical expressions obtained in this space to be able to model the tabular values of the complete elliptic integrals (3) and (7).

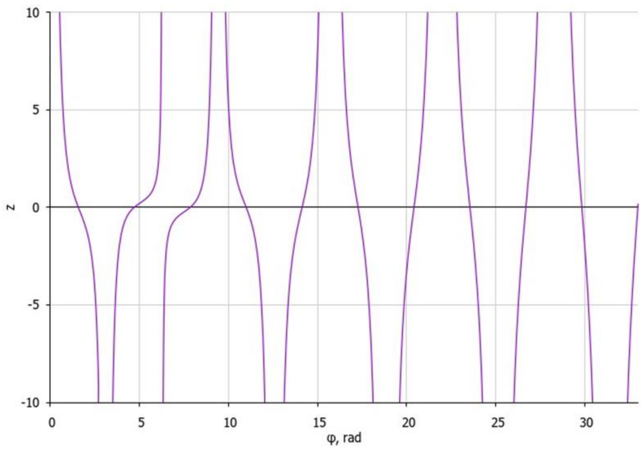

Figure-5. The plots of function (43) for $n=-1$.

4. Result and Discussion

4.1 Integration of the complete elliptic integral of the first kind

Now we will rewrite (36) immediately under the integral sign in the following way:

$$\int \frac{dz}{\sqrt{\tan^2(fz\tan\varphi)+1}} = \int e^{-fz}\left|\cos\left(\frac{z}{\cos\varphi}\right)\right| dz. \quad (44)$$

In order for the integral on the left-hand side of (44) to turn into a complete elliptic integral of the first kind (3), we need to make the following substitution:

$$(k\sin z)^2 = -\tan^2(fz\tan\varphi). \quad (45)$$

Whence

$$k\sin z = i\tan(fz\tan\varphi) = \frac{if}{\sin\varphi}\tan\left(\frac{z}{\cos\varphi}\right). \quad (46)$$

In writing (46), we applied (35).

We also obtain from (46) additional relations that will be needed later:

$$f\cos\varphi = -i\frac{\sin 2\varphi}{2}\frac{k\sin z}{\tan\left(\frac{z}{\cos\varphi}\right)}; \quad (47)$$

$$(f\cos\varphi)^2 = -\left(\frac{\sin 2\varphi}{2}\frac{k\sin z}{\tan\left(\frac{z}{\cos\varphi}\right)}\right)^2. \quad (48)$$

Next, we perform the integration of the right-hand side of (44), taking into account the recurrence of integrals of type

$$\int e^x \sin x\, dx, \quad (49)$$

$$\int e^x \cos x\, dx, \quad (50)$$

and the integration property in the space of tunnel mathematics (34). The result of the integration is as follows:

$$F(z,k) = \int \frac{dz}{\sqrt{1-(k\sin z)^2}} = \frac{1}{\sqrt{1-(k\sin z)^2}} \cdot \frac{\cos\varphi\tan^2\left(\frac{z}{\cos\varphi}\right)}{\tan^2\left(\frac{z}{\cos\varphi}\right)+\left(\frac{\sin 2\varphi}{2}k\sin z\right)^2}\left(\left|\tan\left(\frac{z}{\cos\varphi}\right)\right| - i\frac{\sin 2\varphi}{2}\frac{k\sin z}{\tan\left(\frac{z}{\cos\varphi}\right)}\right). \quad (51)$$

When deriving (51), formulas (47) and (48) were used.

As can be seen from (51), when integrating in the space of tunnel mathematics, the integrand is carried forward, leaving behind a trail of elementary functions. In this case, the resulting expression strongly depends on the azimuthal angle φ (Fig. 3) as a parameter. If $\varphi = 0$, the imaginary part of (51) disappears; if $\varphi = \frac{\pi}{2}$, the full integral $F(z,k)$ disappears completely.

It remains to be seen how well the real and imaginary parts of the expression $F(z,k)$ in (51) model the tabular values of the complete elliptic integral $K(k)$ in (3).

4.1.1 Modeling using the real part of the expression $F(z,k)$

The real part of the expression $F(z,k)$ in (51) looks like this:

$$ReF(z,k) = \frac{1}{\sqrt{1-(k\sin z)^2}} \cdot \frac{\cos\varphi}{\tan^2\left(\frac{z}{\cos\varphi}\right)+\left(\frac{\sin 2\varphi}{2}k\sin z\right)^2}\left|\tan^3\left(\frac{z}{\cos\varphi}\right)\right|. \quad (52)$$

Below are plots of $ReF(z,k)$ for different ranges of values of the modulus k and amplitude z.

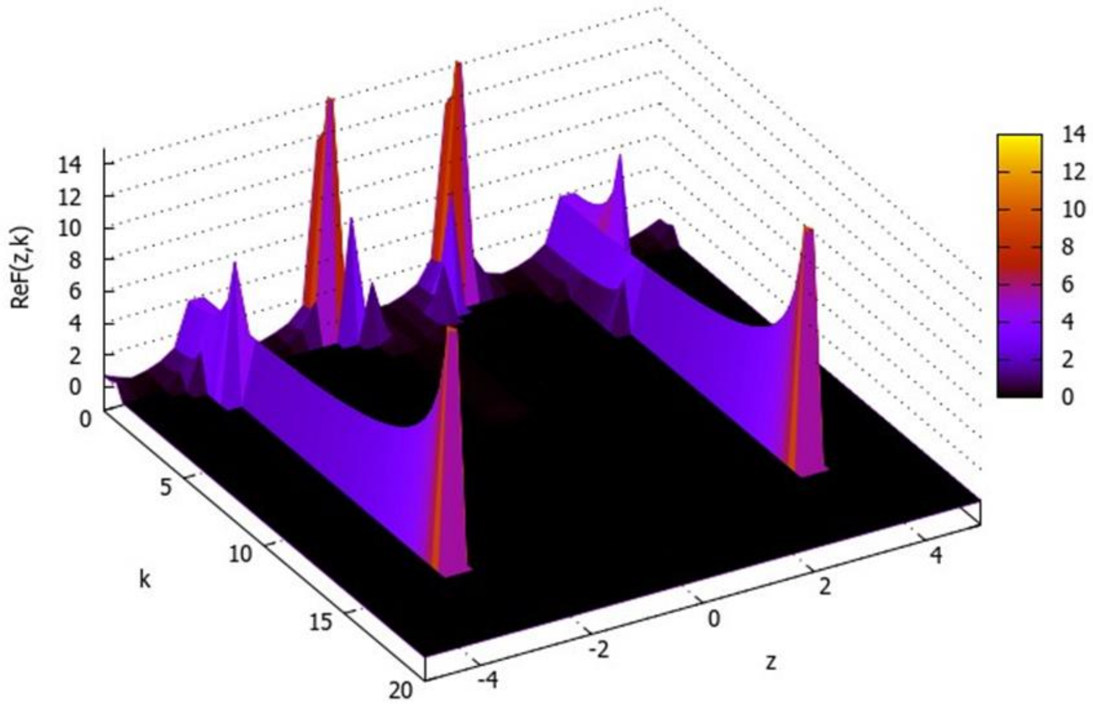

Figure-6. Plot of $ReF(z,k)$ in (52) for $0 < k < 20$; $-4 < z < 4$.

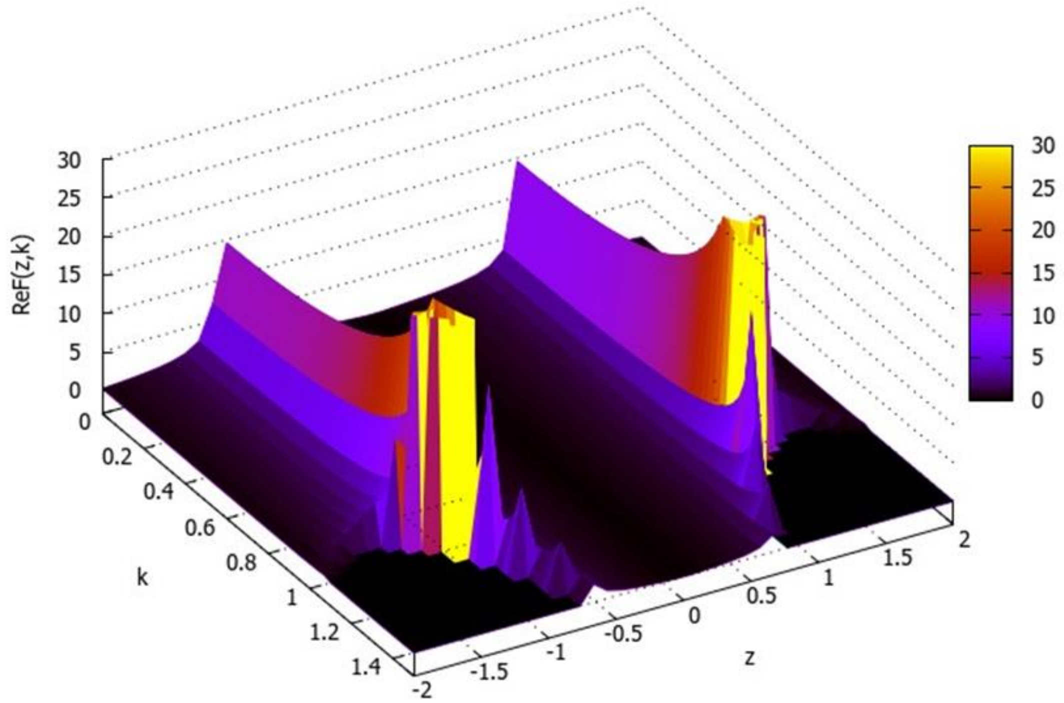

Figure-7. Plot of $ReF(z,k)$ in (52) for $0 < k < 1.5$; $-2 < z < 2$.

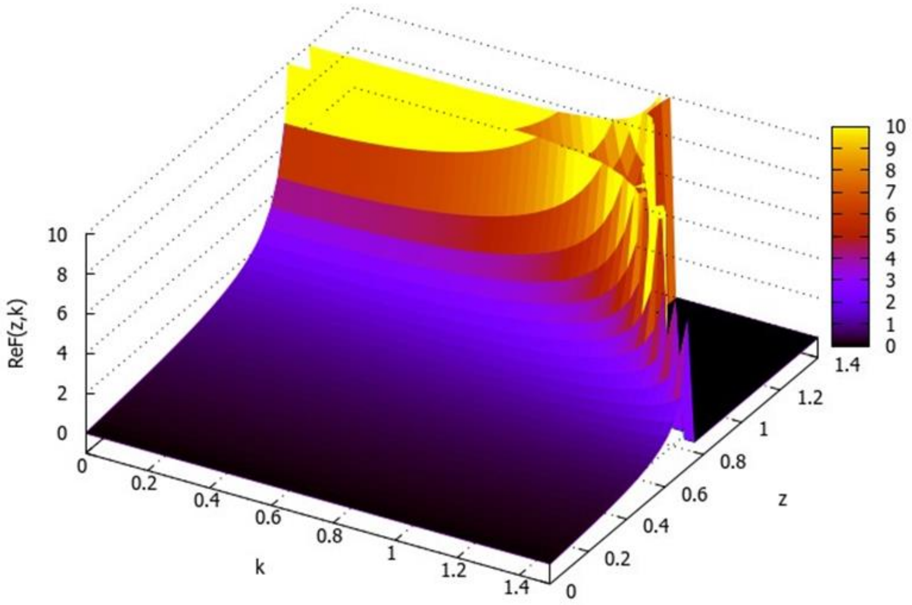

Figure-8. Plot of $ReF(z,k)$ in (52) for $0 < k < 1.5;\ 0 < z < 1.4$.

The plots in Figs. 6 – 8 are built using $\varphi = \frac{\pi}{4} \approx 0.785$. In Fig. 8, a whole set of curves can be clearly seen that can be used to model incomplete elliptic integrals of the first kind (1).

Fig. 9 below shows a plot constructed using the tabular values of *K(k)* in (3) and a plot of $ReF\left(\frac{\pi}{2}, k\right)$ in (52) at $\varphi \approx 0.85\ rad \approx 49°$.

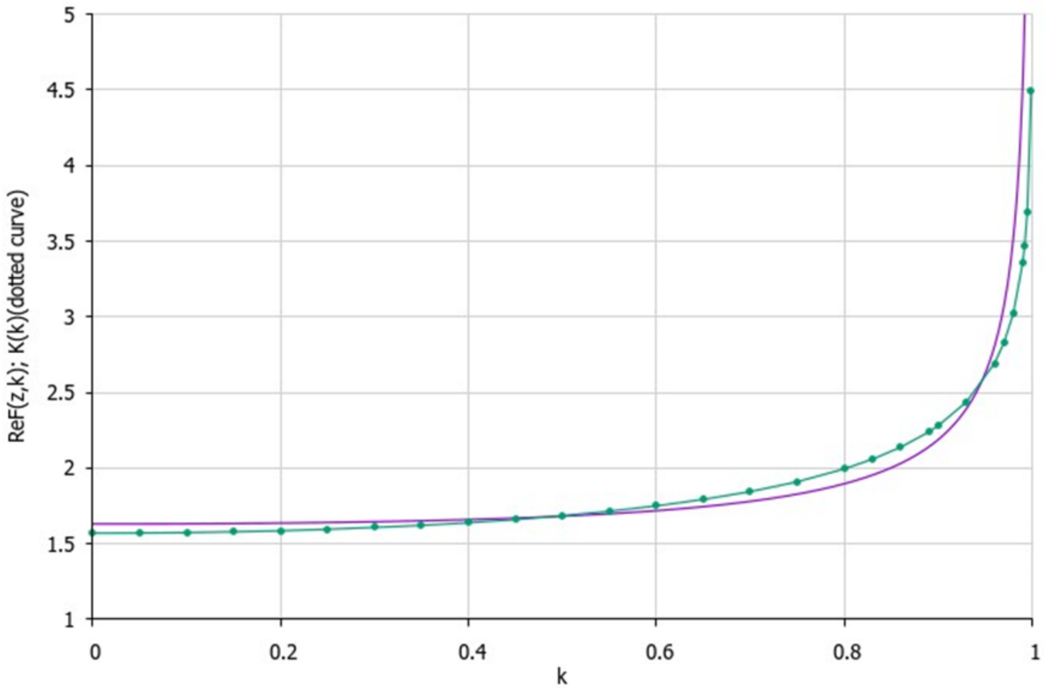

Figure-9. Plot constructed using the tabular values of *K(k)* in (3) (green dotted curve); and a plot of $ReF\left(\frac{\pi}{2}, k\right)$ in (52) at $\varphi \approx 0.85\ rad \approx 49°$ (blue curve; when constructing the plot, 1 was added to expression (52)).

As can be seen from Fig. 9, the modeling is performed with fairly good accuracy. By adjusting the value of the parameter φ, it is possible to reduce the error in the modeling.

Thus, we can conclude that expression (52) at $\varphi \approx 0.85$ is the sum of power series (5).

4.1.2 Modeling using the imaginary part of the expression $F(z, k)$

The imaginary part of the expression $F(z, k)$ in (51) looks like this:

$$ImF(z,k) = -\frac{1}{\sqrt{1-(k\sin z)^2}} \cdot \frac{\cos\varphi}{\tan^2\left(\frac{z}{\cos\varphi}\right)+\left(\frac{\sin 2\varphi}{2}k\sin z\right)^2}\frac{\sin 2\varphi}{2}\ k\sin z\tan\left(\frac{z}{\cos\varphi}\right). \tag{53}$$

Below are plots of $\pm\ ImF(z, k)$ for different ranges of values of the modulus k and amplitude z.

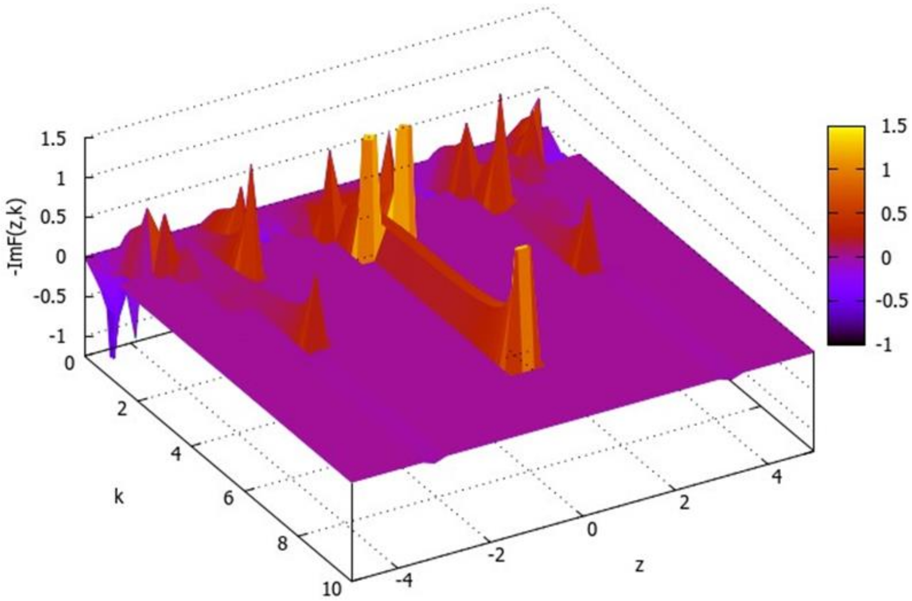

Figure-10. Plot of $-ImF(z, k)$ in (53) for $0 < k < 10$; $-4 < z < 4$.

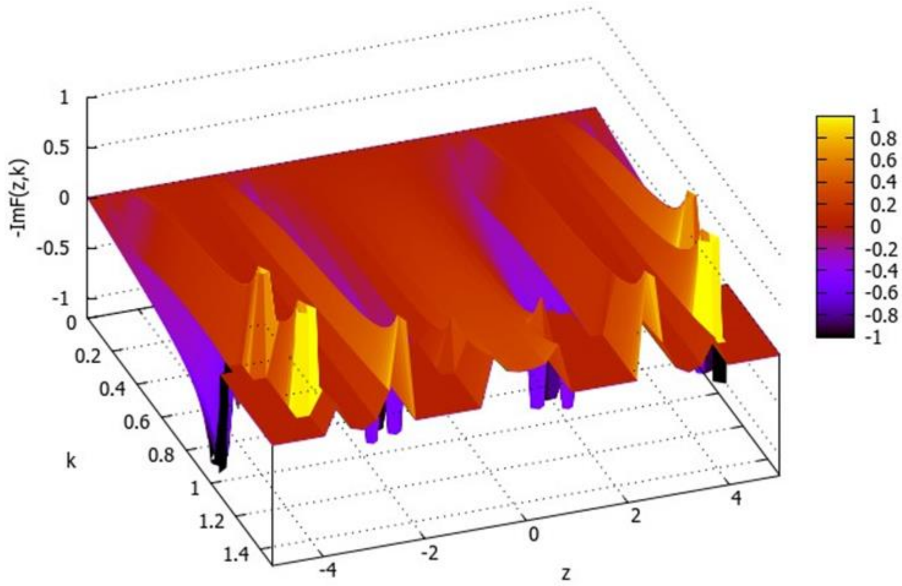

Figure-11. Plot of $-ImF(z, k)$ in (53) for $0 < k < 1.5$; $-4 < z < 4$.

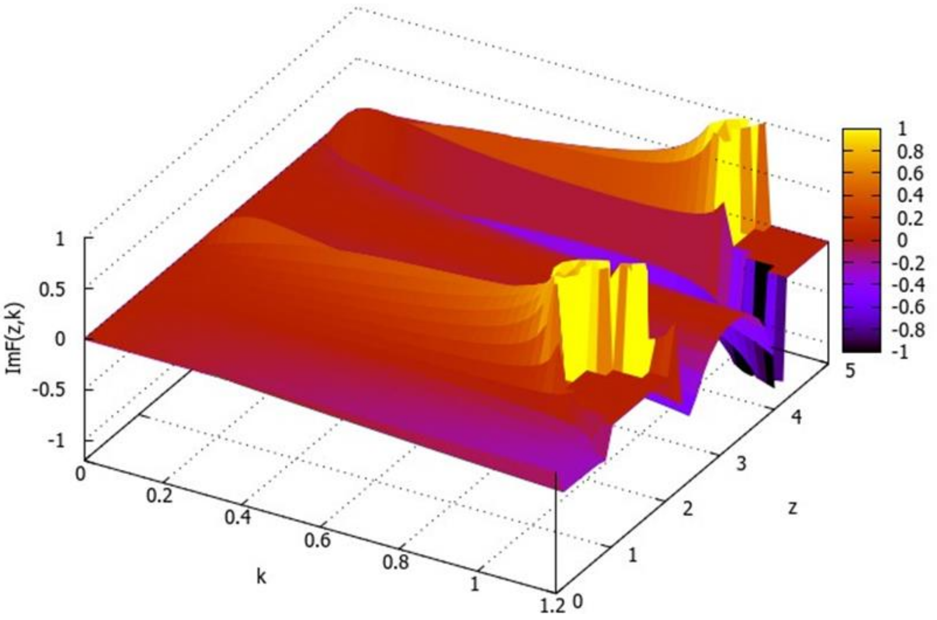

Figure-12. Plot of $ImF(z,k)$ in (53) for $0 < k < 1.2$; $0 < z < 5$.

The plots in Figs. 10 – 12 are built using $\varphi = \frac{\pi}{4} \approx 0.785$. In Fig. 12, a whole set of curves can be clearly seen that can be used to model incomplete elliptic integrals of the first kind (1).

Fig. 13 below shows a plot constructed using the tabular values of *K(k)* in (3) and a plot of $ImF\left(\frac{\pi}{2}, k\right)$ in (53) at $\varphi \approx 0.85\ rad \approx 49°$.

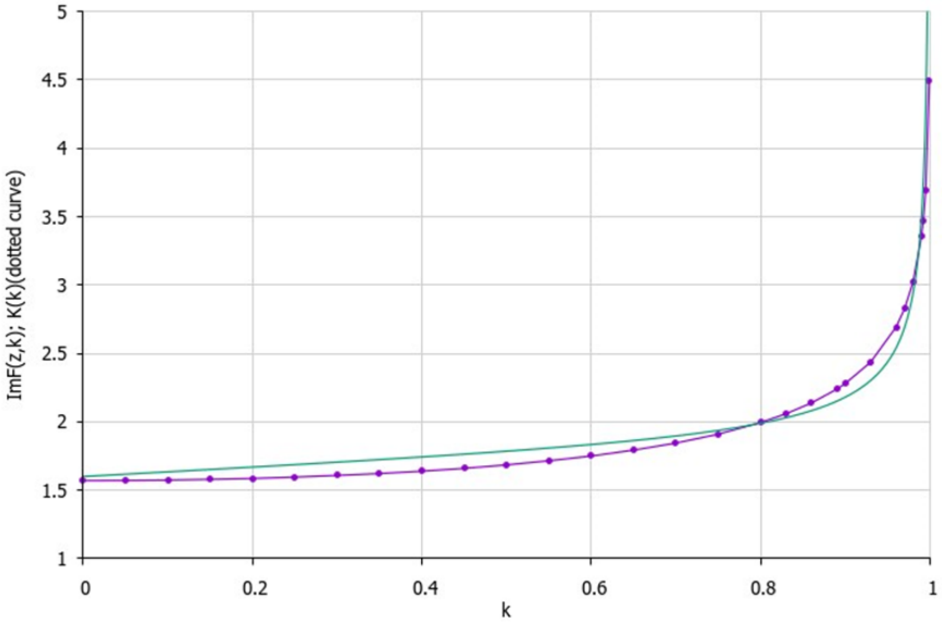

Figure-13. Plot constructed using the tabular values of *K(k)* in (3) (blue dotted curve); and a plot of $ImF\left(\frac{\pi}{2}, k\right)$ in (53) at $\varphi \approx 0.85\ rad \approx 49°$ (green curve; when constructing the plot, 1.6 was added to expression (53)).

As can be seen from Fig. 13, the modeling also is performed with fairly good accuracy. By adjusting the value of the parameter φ, it is possible to reduce the error in the modeling.

As in the case of modeling by means the real part of expression (51), we can conclude that expression (53) at $\varphi \approx 0.85$ also represents the sum of the power series (5).

Based on expressions (52) and (53) we can draw the general conclusion that the nature of the complete elliptic integral of the first kind (3) is closely related to the tangent function.

4.2 Integration of the complete elliptic integral of the second kind

Now we will rewrite (36) immediately under the integral sign in the following way:

$$\int \sqrt{\tan^2(fz\tan\varphi)+1}dz = \int \frac{e^{fz}}{\left|\cos\left(\frac{z}{\cos\varphi}\right)\right|}dz. \quad (54)$$

In order for the integral on the left-hand side of (54) to turn into a complete elliptic integral of the second kind (7), we will use substitution (45), and rewrite expression (46) as follows:

$$k\sin\left(\frac{z}{\cos\varphi}\right) = i\tan\left(fz\frac{\tan\varphi}{\cos\varphi}\right). \quad (55)$$

In the right part of (54) the cosine function is in the denominator. To transfer it to the numerator and use the recurrence of the integrals (49) and (50), we differentiate the expression (55). After which we find the expression for the cosine function:

$$\cos\left(\frac{z}{\cos\varphi}\right) = \frac{1}{k}\,\frac{if\tan\varphi}{\cos^2\left(fz\frac{\tan\varphi}{\cos\varphi}\right)}. \quad (56)$$

Substituting (56) into (54) and performing integration, we obtain the following expression for the elliptic integral of the second kind in the space of tunnel mathematics:

$$E(z,k) = \int\sqrt{1-(k\sin z)^2}\,dz = -(f+2\sin\varphi)\sqrt{1-(k\sin z)^2}\left(1+\left(1-\frac{\cos^2\varphi}{2\tan^2\varphi+\cos^2\varphi}\right)\left(\frac{\cos\varphi}{\tan\varphi}\alpha(\cos\beta+i\sin\beta)-\frac{k}{2\tan\varphi}\cos\left(\frac{z}{\cos\varphi}\right)(\cos\varphi-i\sin\varphi)-1\right)\right); \quad (57)$$

where

$$\alpha = \sqrt{\frac{k}{\tan\varphi}\cos\left(\frac{z}{\cos\varphi}\right)\sqrt{1+\frac{2\sin\varphi}{k\cos\left(\frac{z}{\cos\varphi}\right)}+\left(\frac{k}{\tan\varphi}\cos\left(\frac{z}{\cos\varphi}\right)\right)^{-2}}}; \quad (58)$$

$$\beta = \frac{1}{2}\tan^{-1}\left(-\frac{\sin\varphi}{\cos\varphi+\left(\frac{k}{\tan\varphi}\cos\left(\frac{z}{\cos\varphi}\right)\right)^{-1}}\right). \quad (59)$$

As can be seen from (57), unlike the elliptic integral of the first kind (51), the elliptic integral of the second kind $E(z,k)$ has all three components in the space of tunnel mathematics (10). If $\varphi = 0$, then the elliptic integral of the second kind has only a spatial component:

$$E(z,k) = -f\sqrt{1-(k\sin z)^2}. \quad (60)$$

If $\varphi = \frac{\pi}{2}$, then full integral $E(z,k)$ in (57) disappears. Now let us consider how each of these three components models the complete elliptic integral of the second kind (7).

4.2.1 Modeling using the real part of the expression $E(z,k)$

The real part of the expression $E(z,k)$ in (57) looks like this:

$$ReE(z,k) = -2\sin\varphi\sqrt{1-(k\sin z)^2}\left(1+\left(1-\frac{\cos^2\varphi}{2\tan^2\varphi+\cos^2\varphi}\right)\left(\frac{\cos\varphi}{\tan\varphi}\alpha(\cos\beta+\cos\varphi\sin\beta)+\frac{k\cos\varphi}{2}\cos\left(\frac{z}{\cos\varphi}\right)\left(\cos\varphi-\frac{1}{\tan\varphi}\right)-1\right)\right); \quad (61)$$

where α and β are taken from (58) and (59).

Below are plots of $\pm ReE(z,k)$ for different ranges of values of the modulus k and amplitude z.

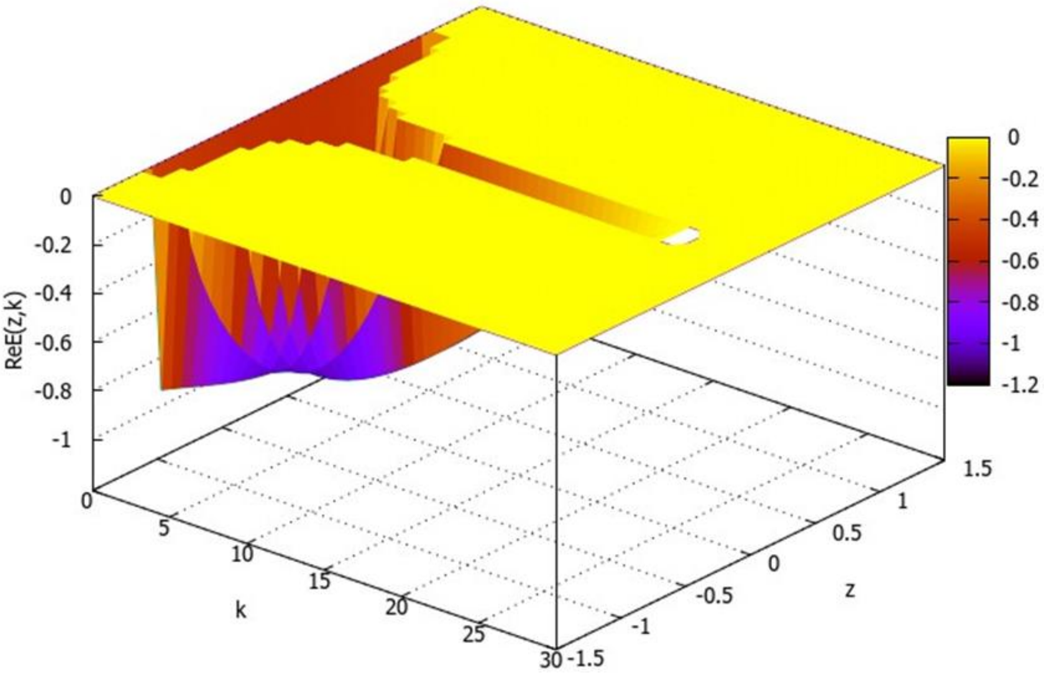

Figure-14. Plot of $ReE(z,k)$ in (61) for $0 < k < 30$; $-1.5 < z < 1.5$.

In Fig. 14 we see a T-shaped profile; in the next figures we will turn it over.

The plots in Figs. 14 – 16 are built using $\varphi = \frac{\pi}{4} \approx 0.785$. In Fig. 16, a whole set of curves can be clearly seen that can be used to model incomplete elliptic integrals of the second kind (6).

Fig. 17 below shows a plot constructed using the tabular values of *E(k)* in (7) and a plot of $-ReE(1.09,k)$ in (61) at $\varphi \approx 0.785\ rad = 45°$. In this case, we determined the value of amplitude *z* from the equality

$$z = \frac{\pi}{2}\cos\varphi = 1.57 \cdot 0.7 = 1.09.$$

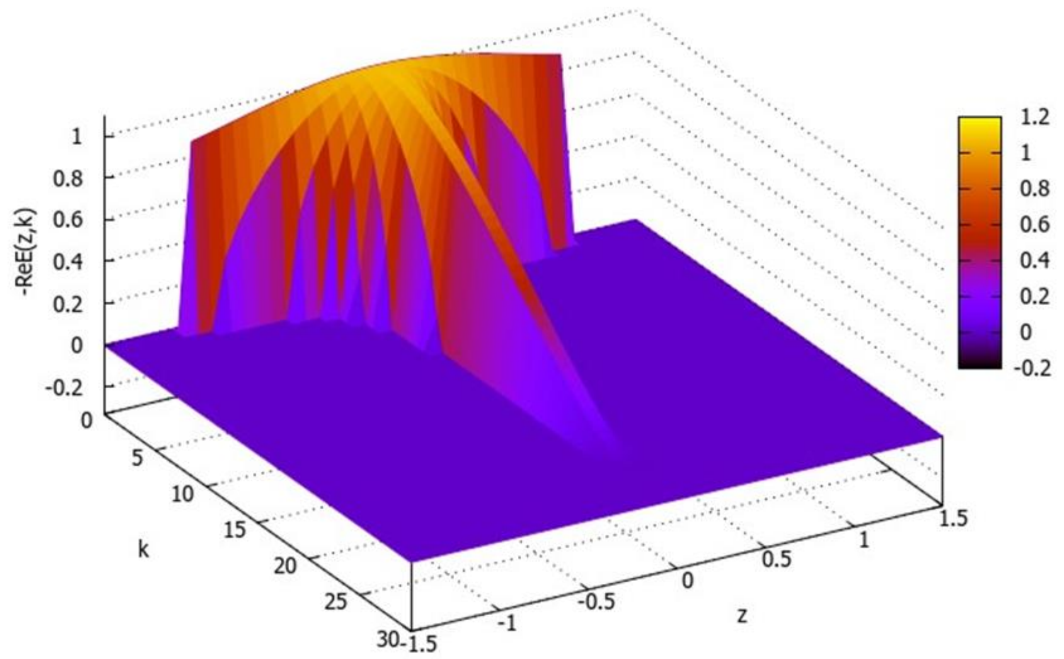

Figure-15. Plot of $-ReE(z,k)$ in (61) for $0 < k < 30$; $-1.5 < z < 1.5$.

The values of the modulus k can extend much further than those shown in Fig. 15; however, the values of the amplitude z in this case are very close to zero (see Fig. 18 for the spatial component).

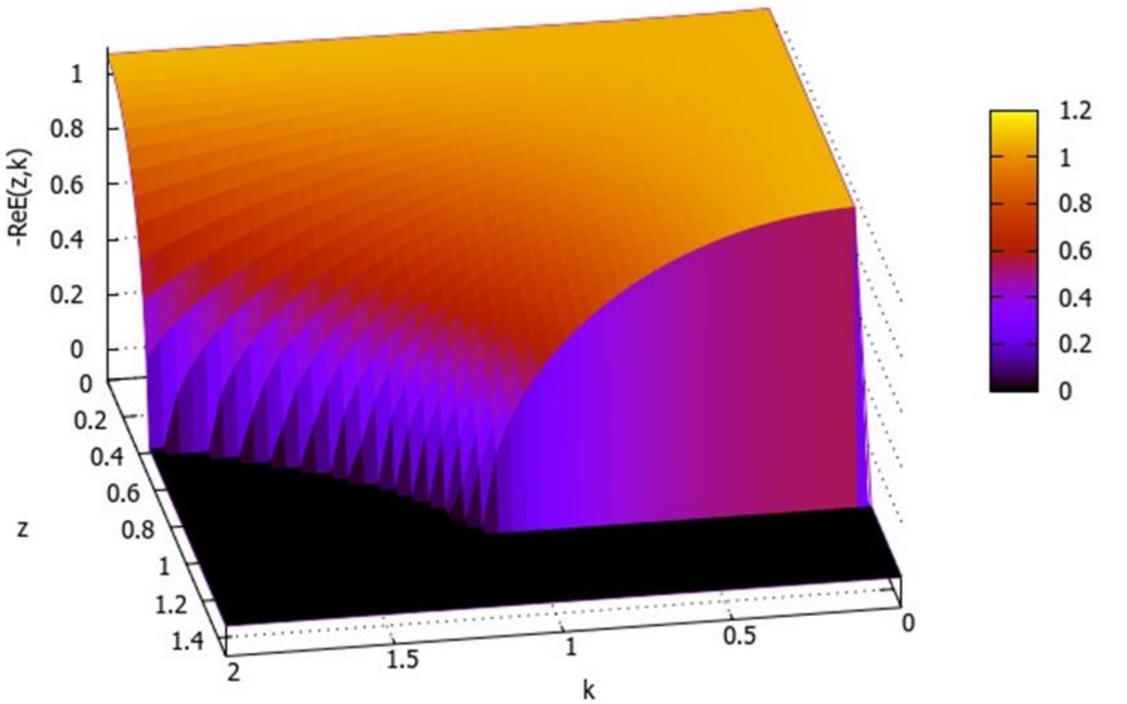

Figure-16. Plot of $-ReE(z,k)$ in (61) for $0 < k < 2$; $0 < z < 1.5$.

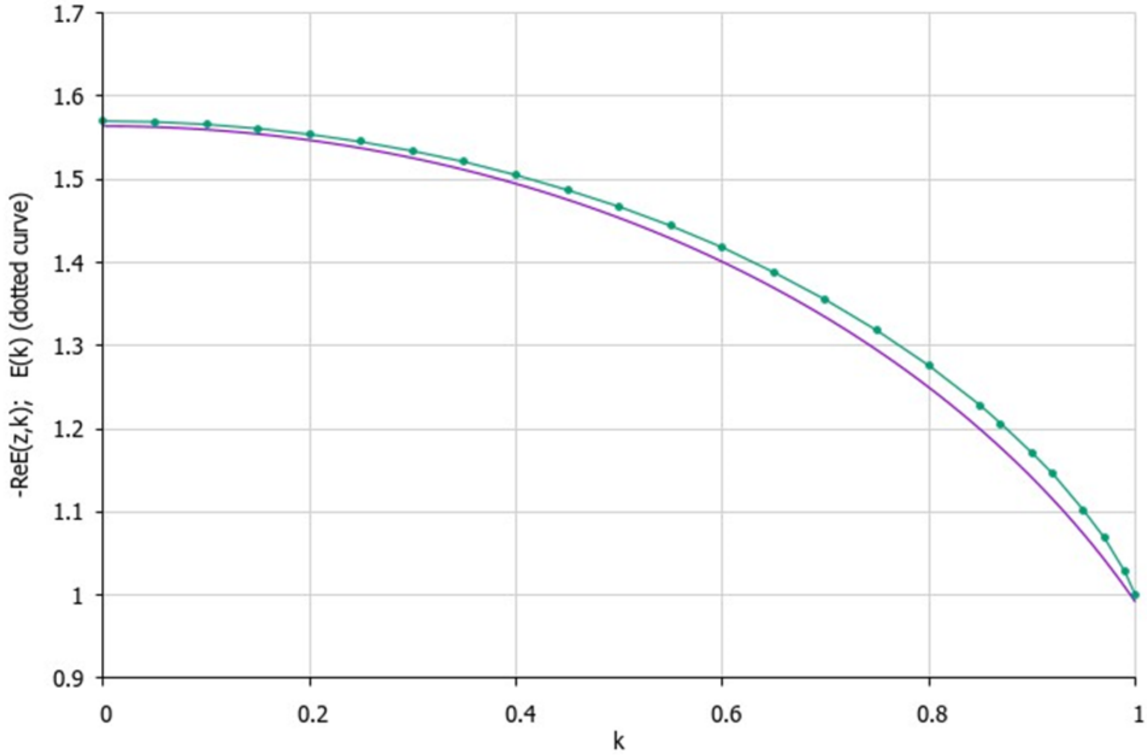

Figure-17. Plot constructed using the tabular values of *E(k)* in (7) (green dotted curve); and a plot of $-ReE(1.09, k)$ in (61) at $\varphi \approx 0.785\ rad = 45°$ (blue curve; when constructing the plot, 0.5 was added to expression (61)).

As can be seen from Fig. 17, the modeling is performed with fairly good accuracy. By adjusting the value of the parameter φ, it is possible to reduce the error in the modeling.

Thus, we can conclude that expression (61) at $\varphi \approx 0.785$ is the sum of power series (9).

4.2.2 Modeling using the spatial part of the expression $E(z, k)$

The spatial part of the expression $E(z, k)$ in (57) is very similar to the real part, so we first consider it and not the imaginary component:

$$FantE(z,k) = -\sqrt{1-(k\sin z)^2}\left(1+\left(1-\frac{\cos^2\varphi}{2\tan^2\varphi+\cos^2\varphi}\right)\left(\frac{\cos\varphi}{\tan\varphi}\left(\alpha\cos\beta-\frac{k}{2}\cos\left(\frac{z}{\cos\varphi}\right)\right)-1\right)\right); \quad (62)$$

where α and β are taken from (58) and (59).

Below are plots of $\pm FantE(z, k)$ for different ranges of values of the modulus *k* and amplitude *z*.

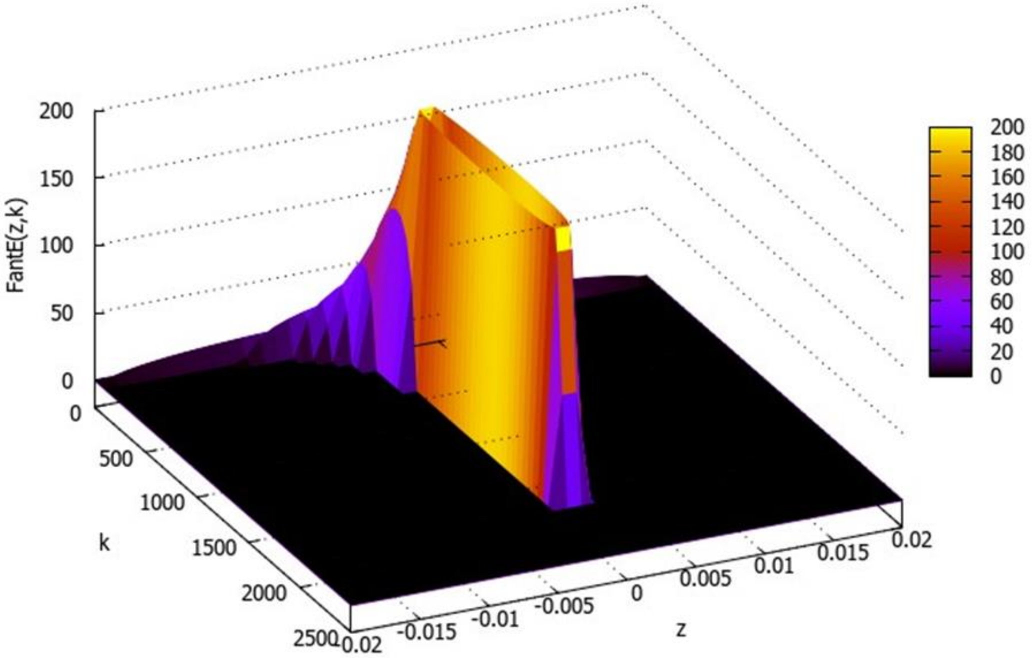

Figure-18. Plot of $FantE(z, k)$ in (62) for $0 < k < 2500$; $-0.02 < z < 0.02$.

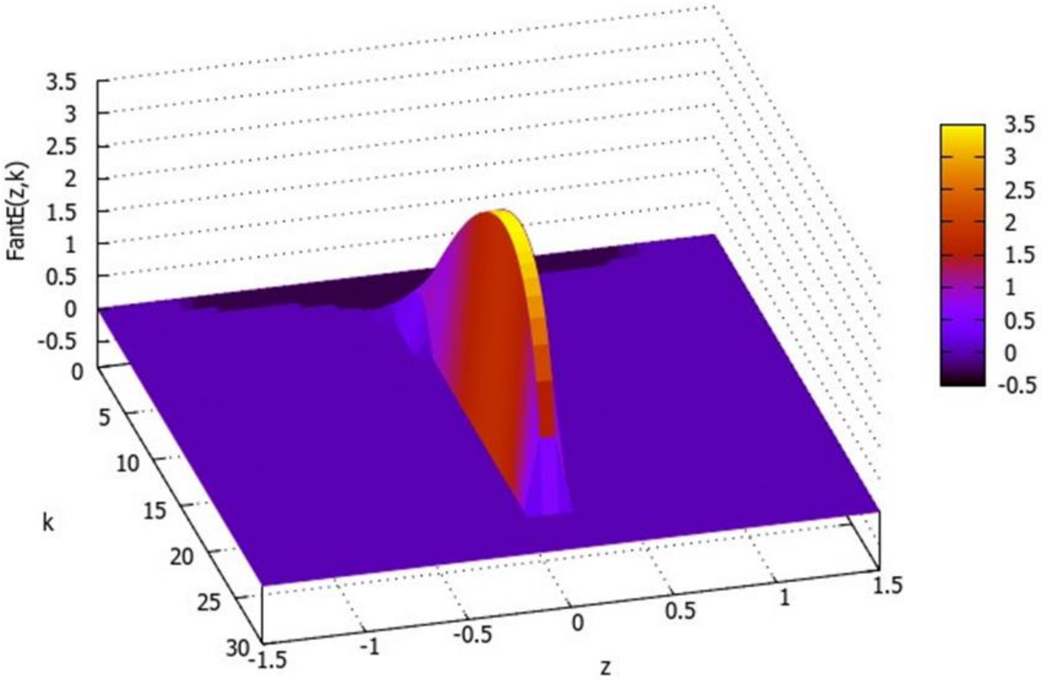

Figure-19. Plot of $FantE(z, k)$ in (62) for $0 < k < 30$; $-1.5 < z < 1.5$.

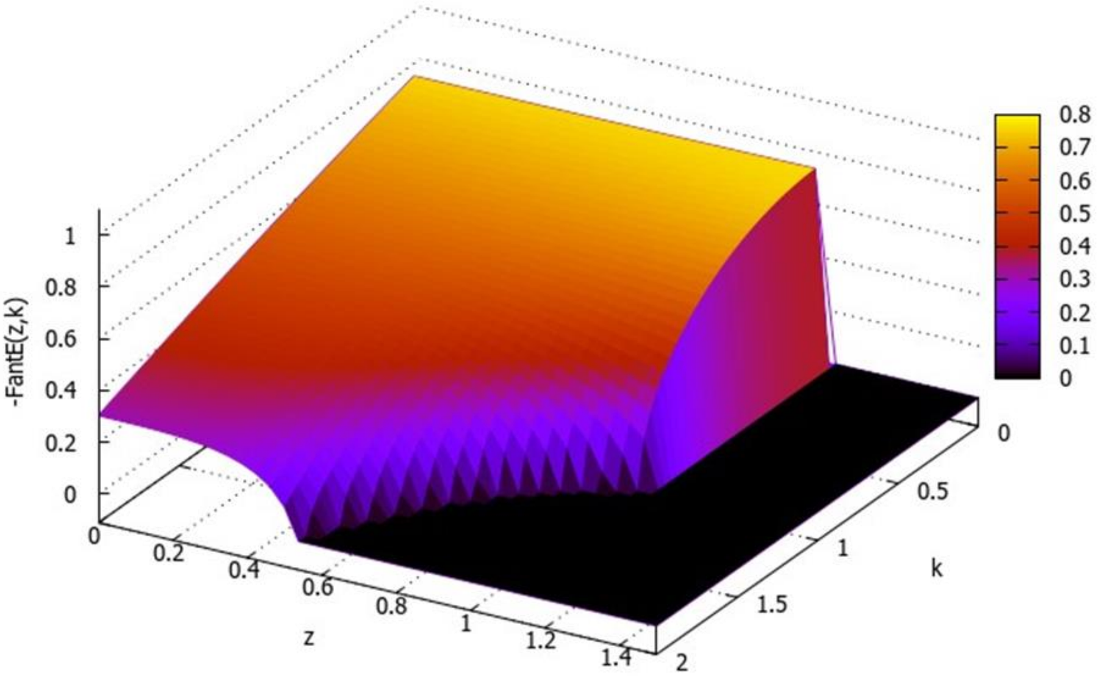

Figure-20. Plot of $-FantE(z,k)$ in (62) for $0 < k < 2;\ 0 < z < 1.5$.

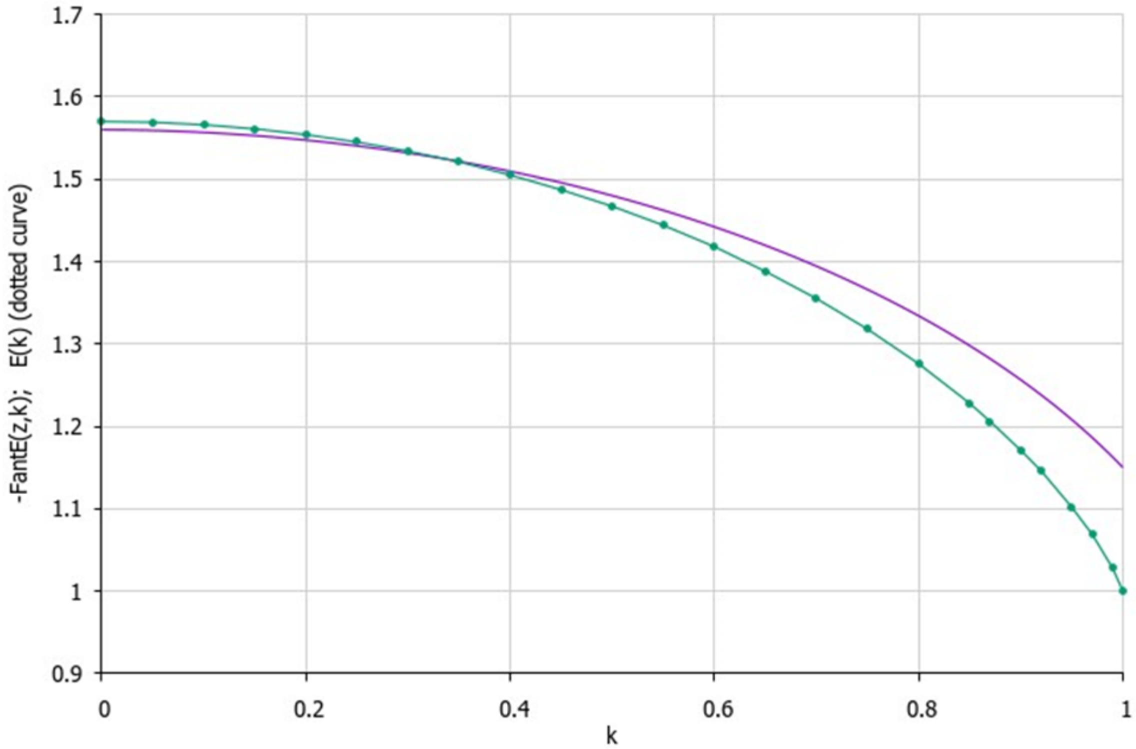

Figure-21. Plot constructed using the tabular values of *E(k)* in (7) (green dotted curve); and a plot of $-FantE(1.09, k)$ in (62) at $\varphi \approx 0.785\ rad = 45°$ (blue curve; when constructing the plot, 0.8 was added to expression (62)).

The plots in Figs. 18 – 20 are built using $\varphi = \frac{\pi}{4} \approx 0.785$. In Fig. 20, a whole set of curves can be clearly seen that can be used to model incomplete elliptic integrals of the second kind (6).

Fig. 21 shows a plot constructed using the tabular values of *E(k)* in (7) and a plot of $-FantE(1.09, k)$ in (62) at $\varphi \approx 0.785\ rad = 45°$. In this case, we determined the value of amplitude *z* from the equality

$z = \frac{\pi}{2} \cos\varphi = 1.57 \cdot 0.7 = 1.09.$

Analyzing Fig. 21, we can conclude that modeling using the spatial part of the expression $E(z, k)$ in (57) for the value of the parameter $\varphi = \frac{\pi}{4} \approx 0.785$ is unsatisfactory.

4.2.3 Modeling using the imaginary part of the expression $E(z, k)$

The imaginary part of the expression $E(z, k)$ in (57) looks like this:

$$ImE(z, k) = -\cos\varphi \sqrt{1 - (k \sin z)^2} \left(1 - \frac{\cos^2\varphi}{2\tan^2\varphi + \cos^2\varphi}\right) \left(\cos\varphi\, \alpha \sin\beta + \frac{k}{2} \sin\varphi \cos\left(\frac{z}{\cos\varphi}\right)\right); \quad (63)$$

where α and β are taken from (58) and (59).

Below are plots of $-ImE(z, k)$ for different ranges of values of the modulus *k* and amplitude *z*.

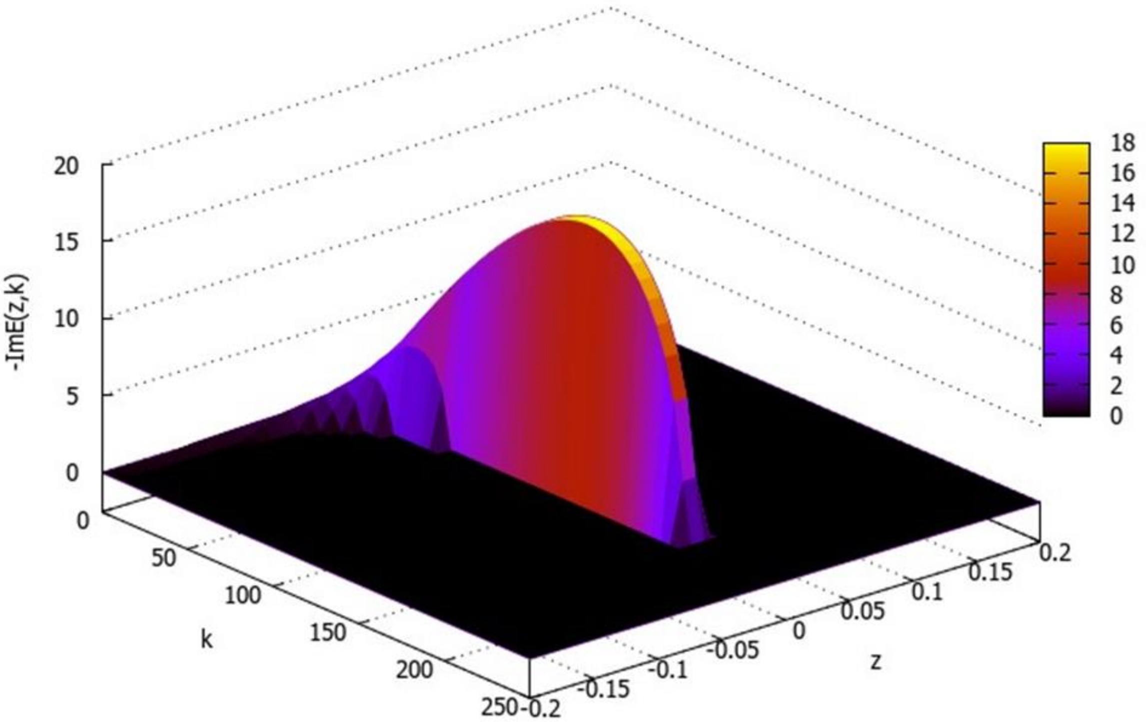

Figure-22. Plot of $-ImE(z, k)$ in (63) for $0 < k < 250$; $-0.2 < z < 0.2$.

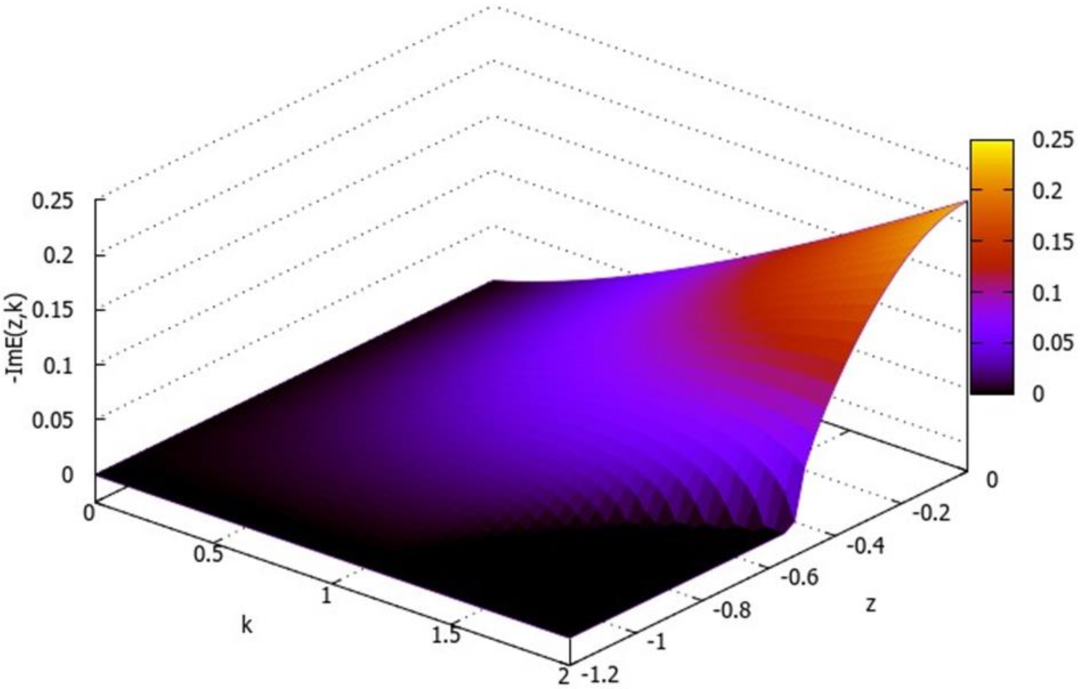

Figure-23. Plot of $-ImE(z,k)$ in (63) for $0 < k < 2$; $-1.2 < z < 0$.

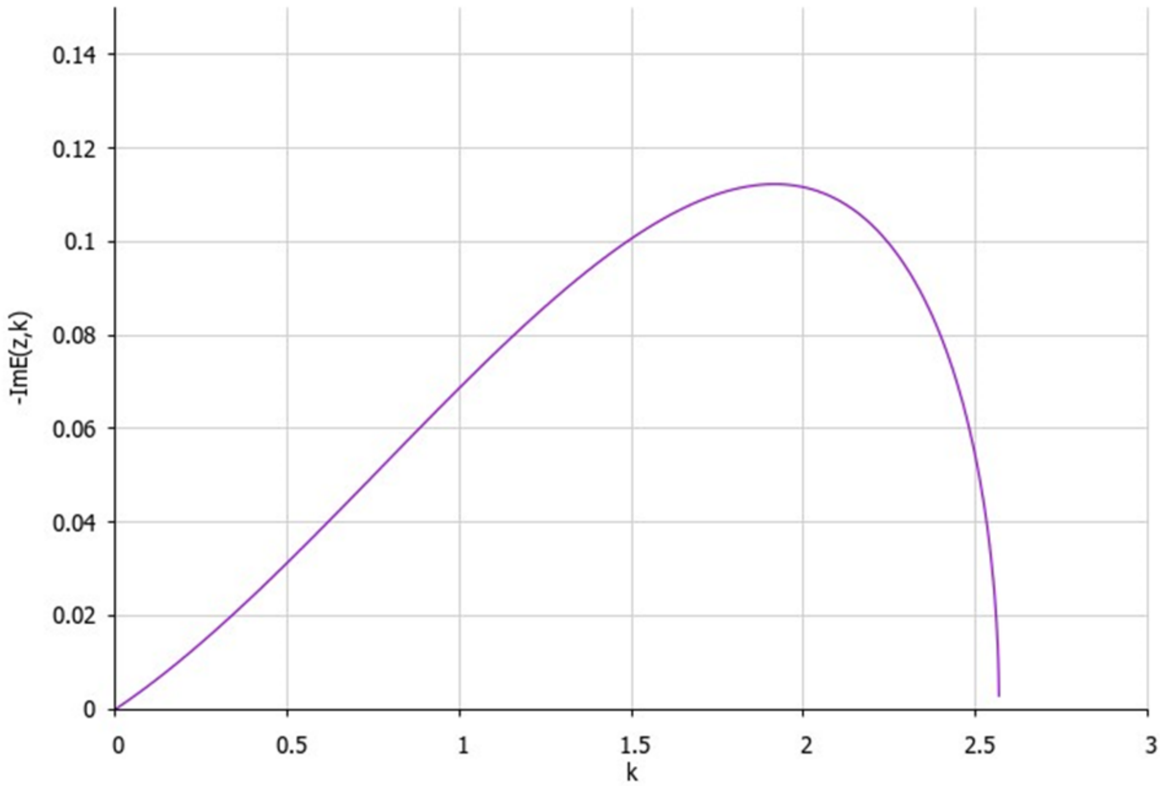

Figure-24. Plot of $-ImE(1.09,k)$ in (63) at $\varphi \approx 0.785\ rad = 45°$.

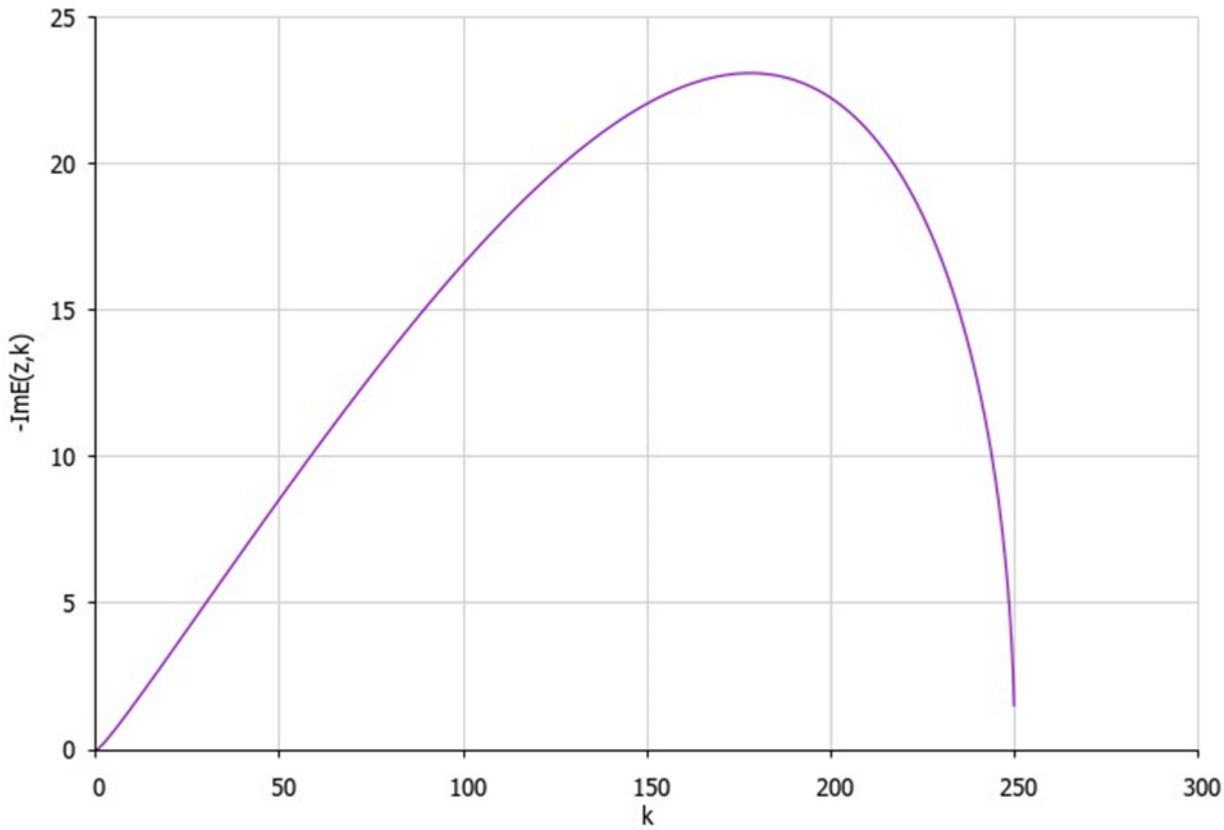

Figure-25. Plot of $-ImE(-0.004, k)$ in (63) at $\varphi \approx 0.785\ rad = 45°$.

The plots in Figs. 22 – 25 are built using $\varphi = \frac{\pi}{4} \approx 0.785$.

Fig. 24 shows a plot of $-ImE(1.09, k)$ in (63) at $\varphi \approx 0.785\ rad = 45°$. In this case, we also determined the value of amplitude *z* from the equality

$$z = \frac{\pi}{2}\cos\varphi = 1.57 \cdot 0.7 = 1.09.$$

Analyzing Fig. 24, we see that the plot of the imaginary part of the expression $E(z, k)$ in (57) for the value of the parameter $\varphi = \frac{\pi}{4}$ has nothing in common with the plot for the complete elliptic integral *E(k)* in Fig. 2.

Fig. 25 shows a plot of $-ImE(-0.004, k)$ in (63) at $\varphi \approx 0.785\ rad = 45°$. It shows that when the amplitude *z* decreases approximately by 100 times, the values of the modulus *k* increase linearly.

5. Conclusion

Integration of complete elliptic integrals of the first and second kind in the space of tunnel mathematics brings the integrand forward, leaving behind it a trail of elementary functions. The plots of the resulting analytical expressions simulate with fairly good accuracy the plots of both integrals, constructed using tabular values. In order to use the expressions for both integrals simultaneously in calculations, it is necessary to select the corresponding value of the parameter φ. This may cause some inconvenience. The resulting expressions are not satisfied in the entire space of tunnel mathematics. They hold in the *xy*-plane, on the *z*-axis, and also on some lines or filaments in this space. However, even this is enough for at least one of the components of the expression for each of the integrals to be able to model tabular values of the corresponding integral well. Our results show that the nature of the complete elliptic integral of the first kind is closely related to the tangent function. The obtained analytical expressions for complete elliptic integrals of the first and second kind can also be used to model the corresponding incomplete ones, but this is already the topic of another study.

6. References

[1] Abramowitz, M. and Stegun, I. A. (Eds.). "Elliptic Integrals." Ch. 17 in Handbook of Mathematical Functions with Formulas, Graphs, and Mathematical Tables, 9th printing. New York: Dover, pp. 587-607, 1972.
[2] Arfken, G. "Elliptic Integrals." §5.8 in Mathematical Methods for Physicists, 3rd ed. Orlando, FL: Academic Press, pp. 321-327, 1985.
[3] Hancock, H. Elliptic Integrals. New York: Wiley, 1917.
[4] Kármán, T. von and Biot, M. A. Mathematical Methods in Engineering: An Introduction to the Mathematical Treatment of Engineering Problems. New York: McGraw-Hill, p. 121, 1940.
[5] Prasolov, V. and Solovyev, Y. Elliptic Functions and Elliptic Integrals. Providence, RI: Amer. Math. Soc., 1997.
[6] Prudnikov, A. P.; Brychkov, Yu. A.; and Marichev, O. I. Integrals and Series, Vol. 1: Elementary Functions. New York: Gordon & Breach, 1986.
[7] Byrd, P. F.; Friedman, M.D. (1971). Handbook of Elliptic Integrals for Engineers and Scientists (2nd ed.). New York: Springer-Verlag.
[8] Carlson, B. C. (2010), "Elliptic integral", in Olver, Frank W. J.; Lozier, Daniel M.; Boisvert, Ronald F.; Clark, Charles W. (eds.), NIST Handbook of Mathematical Functions, Cambridge University Press.
[9] Erdélyi, Arthur; Magnus, Wilhelm; Oberhettinger, Fritz; Tricomi, Francesco G. (1953). Higher transcendental functions. Vol II. McGraw-Hill Book Company, Inc., New York-Toronto-London.
[10] Gradshteyn, Izrail Solomonovich; Ryzhik, Iosif Moiseevich; Geronimus, Yuri Veniaminovich; Tseytlin, Michail Yulyevich; Jeffrey, Alan (2015) [October 2014]. "8.1.". In Zwillinger, Daniel; Moll, Victor Hugo (eds.). Table of Integrals, Series, and Products. Translated by Scripta Technica, Inc. (8 ed.). Academic Press, Inc.
[11] Wikipedia. Elliptic integral.
[12] Lavrentiev M. Méthodes de la théorie des fonctions d'une variable complexe / M. Lavrentiev, B. Chabat: traduit du russe. — Moscou: Mir, 1972. — 728 p.
[13] Oleh G. Shvydkyi. (2022). Tensor foundations of tunnel mathematics, Preprint, https://doi.org/10.21203/rs.3.rs-2827573/v1
[14] Landau and Lifshitz (1987). Fluid Mechanics, Course of Theoretical Physics, Volume 6, Second English Edition, Pergamon Press, pp. 95-135.

7. Conflict of Interest

The author declares no competing conflict of interest.

8. Funding

No funding was received to support this study.